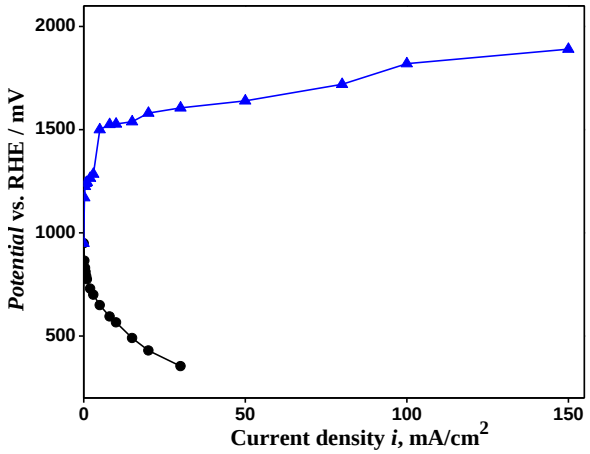

Fig. 3. Charge (▲) and discharge (●) voltages of an optimized bifunctional GDE at different current densities in a homemade 10 cm^2 cell.

The cycling test was performed applying a current density of ±10 mA/cm^2 during 7 h of charge and 6 h of discharge. The cut-off voltages were set at 2.5 V at charge (C) and 0.5 V at discharge (D), respectively (Fig.4) after the first cycles where the C/D voltages were beyond these limits. This situation most likely induced Zn passivation reflected by the subsequent decrease in capacity.

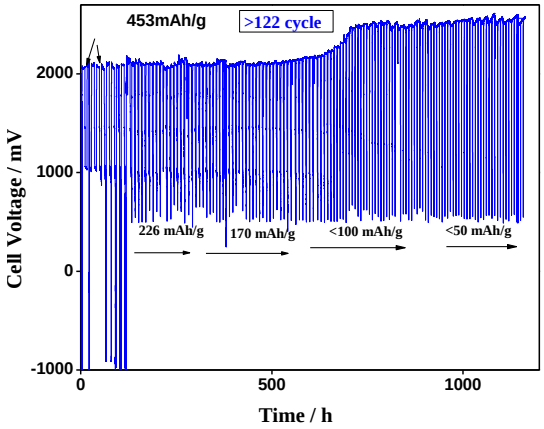

Fig. 4. Long-term cycling of homemade Zn/Air cell at 10 mA/cm^2

The impedance measurements were carried out using a Solartron 1260 Frequency Response Analyzer in the frequency range 1 kHz – 10 mHz with density of 5 points per decade at applied DC current of 10 mA and amplitude of the AC signal of 2.5 mA during both charge and discharge modes. They were performed after the 20^{th} cycle and at the end of the cell life at similar state of charge or discharge for characterization of both the electrodes and cell behavior. For convenience, the impedance measurements of the electrodes were related to the cell voltage, measured before the AC perturbation. Preliminary screening performed before and after the impedance experiments registered insufficient voltage changes, which could be ignored.

RESULTS AND DISCUSSIONS

The volt-ampere characteristic (VAC) is a key feature of any electrochemical power source. It covers the entire operating range and reflects the set of dominant phenomena that govern a process. Thus, VAC gives the main fundamental and simplest description of the cell performance in a given moment of the test. VAC depends on the operating conditions and degradation state. For batteries the state of charge/discharge should be also taken into account. Therefore, at constant working conditions the changes in the VAC may serve as performance indicator to estimate the state of health (SoH) and the degradation rate. For deeper insight into the phenomena and mechanisms the VAC analysis is combined with impedance measurements in selected working points [16].

Fig. 5 represents VAC of the homemade Zn-air cell at a given state during discharge after 20 previous charge/discharge cycles. Generally, the volt-ampere curve has three distinct areas: (*i*) an activation zone at low current (segment I in Fig. 5), followed by (*ii*) a transport zone with linear behavior (segment II in Fig. 5) and (*iii*) a diffusion restriction zone at high current (not presented in Fig. 5). A working point (WP) at 10 mA was selected (triangle in Fig.5) to perform the impedance measurements of the Zn-Air cell in both full- and half-cell configuration. Due to its position in the kink of segments I and II in the voltage-current curve, the measured impedance can ensure information about both the charge transfer, which depends on the electrode catalytic activity, and the transport hindrances.

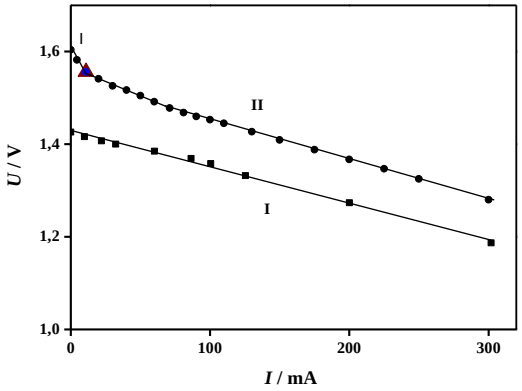

Fig. 5. Volt-ampere characteristic of a Zn-air cell in discharge regime: (●) full cell configuration; (■) half-cell configuration of gas diffusion electrode (GDE).

The VAC of the GDE recorded during discharge shows a linear behavior (Fig. 5.). This is

characteristic of electrodes operating under the domination of transport limitations. The VAC comparison with the full cell performance suggests that the activation losses come mainly from the Zn electrode. This hypothesis is confirmed by the impedance measurements presented in Fig. 6.

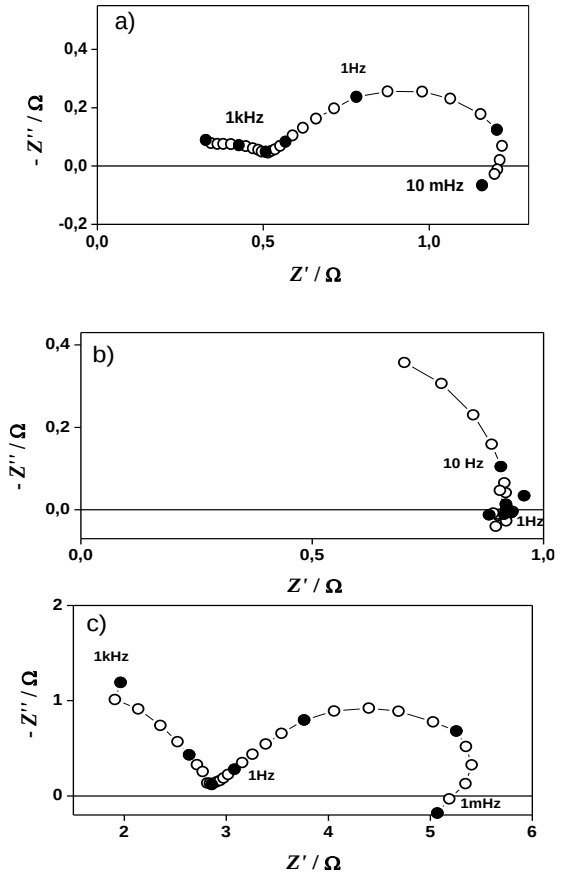

Fig. 6. Impedance diagrams for: a) GDE, b) Zn electrode and c) full-cell during discharge (1,6 V).

The impedance diagram of the GDE (Fig. 6a) is characterized by a well-defined low frequency arch corresponding to bounded transport limitations, while that for the Zn electrode (Fig. 6b) exhibits the domination of the charge transfer semicircle. The impedance of the full cell combines the two characteristic impedance shapes in the high and in the low frequency range, respectively. A significant increase of the resistance is also observed (Fig. 6c). The state of discharge (SoD) influences weakly the anode reaction. The inductive complicated shape in the low frequency range, which is typical for impedance of batteries, usually marks the formation of a new phase [17].

The impedance diagrams for the full cell and for the two electrodes during charge are also well defined (Fig. 7). The charge transfer resistance of the zinc electrode decreases about 3 times, which obviously influences also the cell resistance (Fig. 7b). This asymmetry during charge and discharge may be due to the screening effect of the teflonized anode surface.

The volt-ampere characteristic and impedance measurements in full cell configuration performed at the end of the cell life (after 120 C/D cycles) showed strongly deteriorated behavior (Fig. 8). The resistance registered by impedance was about 10 times higher in comparison to that after the 20th C/D cycle.

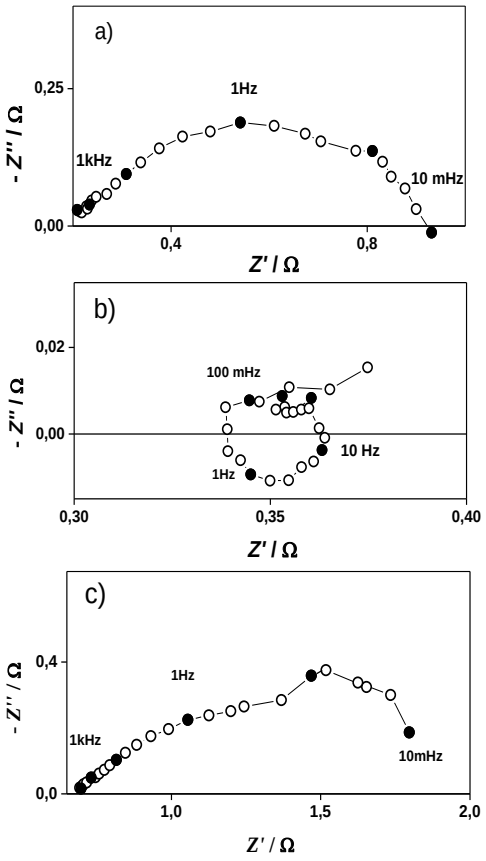

Fig. 7. Impedance diagrams for: a) GDE, b) Zn electrode and c) full-cell during charge (1,9 V).

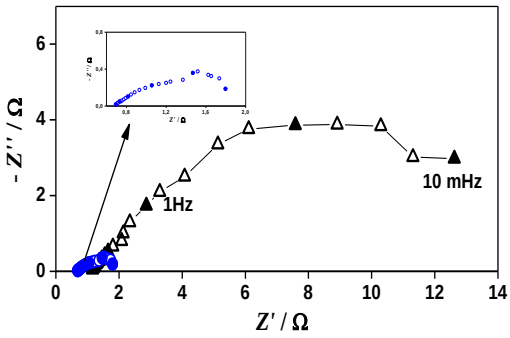

Fig. 8. Impedance characteristics of full cell during charge (about 1,8 V) after the 20th cycle (●) and after the last (120th) cycle (▲).

The subsequent measurement of the Zn electrode failed, due to obviously the entire Zn dissolution and total loss of contacts with the current collector (visually confirmed after opening the cell). It is interesting to note that a lower

resistance was registered for the measurements in full cell configuration after the failure of the Zn electrode (Fig. 9), which can be explained with a change of the system, since in practice the Zn electrode was replaced by the stainless steel current collector.

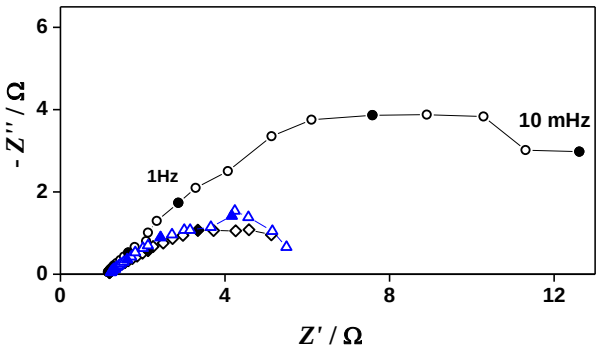

Fig. 9. Impedance of full cell during charge after the 120th discharge: before (●) and after (▲, ♦) the failure of the Zn electrode.

After opening the homemade cell, it could be seen that while the zinc electrode was totally dissolved, the GDE was in good condition (Fig. 10). The replacement of the damaged Zn electrode with a new one and refreshment of the electrolyte ensured more than 50 additional C/D cycles at 10 mA/cm^2.

Fig. 10. Gas diffusion electrode before and after 120 C/D cycles.

CONCLUSIONS

These preliminary results demonstrate the applicability of EIS for performance studies of Zinc-air rechargeable cells. The measurements can be carried out in half-cell and full-cell configuration during charge or discharge. This versatility ensures information about the behavior and influence of the cell components thus determining the rate limiting step and its position in the cell. Comparison of volt-ampere characteristics combined with periodic impedance measurements during battery cycling can bring to a deeper insight into the degradation mechanisms. Getting such knowledge, Zinc-air cells can be further optimized in terms of performance and cycle life.

Acknowledgements: *The research leading to these results has received funding from the European commission by the project "Zinc Air Secondary innovative nanotech based batteries for efficient energy storage" (ZAS) of the Horizont 2020: H2020-NMP-2014 Project number: 646186.*

REFERENCES

1. A. Kaisheva in: Z. Stoynov and D. Vladikova (Eds.), Portable and Emergency Energy Sources, Marin Drinov Academic Publishing House, Sofia, p. 301, (2006).
2. P. Gu, M. Zheng, Q. Zhao, X. Xiao, H. Xue, H. Pang, *J. Mater. Chem. A*, **5**, 7651 (2017) DOI: 10.1039/ C7TA01693J.
3. J. Fu, Z. P. Cano, M. G. Park, A. Yu, M. Fowler, Z. Chen, *Adv. Mater*. 29, **7** (2016). DOI: 10.1002/adma. 201604685.
4. EU funded H2020 project „Zinc-Air Secondary innovative nanotech based batteries for efficient energy storage" ZAS (GA 646186) (http://sintef.no/projectweb/zas/).
5. A. R. Mainar, L. C. Colmenares, J. A. Blázquez, I. Urdampilleta, Int. J. Energy Res., **42**, 903 (2018). doi.org/10.1002/er.3822.
6. A. R. Mainar, L. C. Colmenares, O. Leonet, F. Alcaide, J. Iruin, S. Weinberger, V. Hacker, E. Iruin, I. Urdanpilleta, J. A. Blazquez, *Electrochim.Acta*, **217,** 80 (2016). doi.org/10.1016/j.electacta.2016.09.052.
7. E. Davaria, D. Ivey, *Sustainable Energy Fuels*, **2**, 39, (2018).
8. S. Velraja, J. Zhua, ECS Meeting Abstracts, 232nd ECS Meeting, MA2017-02 National Harbor, Maryland (2017).
9. A. R. Mainar, L. C. Colmenares, M. Juel, E. Sheridan, J. A. Blázquez, I. Urdampilleta, Proc. II Metal-air Batteries International Congress, Santander (2016).
10. Z. Stoynov, D. Vladikova, Impedance Spectroscopy of Electrochemical Power Sources in: U. Garche (Ed.) Encyclopedia of Electrochemical Power Sources, Elsevier, p. 632, 2009.
11. D. Vladikova, Z. Stoynov, G. Raikova, A. Thorel, A. Chesnaud, J. Abreu, M. Viviani, A. Barbucci, Z. Ilhan, P. Carpanese, S. Presto, Proc. 15th European Fuel Cell Forum 2011, 28 June – 1 July 2011, Lucerne, Switzerland, Ch. 18/B1205, p. 1, (2011).
12. Z. Stoynov, D. Vladikova, E. Mladenova, *J. Solid State Electrochem*., **17**, 555, (2013). DOI: 10.1007/s10008-012-1916-z.
13. B. Abrashev, D. Uzun, H. Hristov, D. Nicheva, K. Petrov, Adv. Natural Science: Theory & Applications, **4**, 65 (2015)
14. H. M. A. Amin, H. Baltruschat, D. Wittmaier, K. A. Friedrich, *Electrochim.Acta*, **151**, 332 (2015). DOI: doi.org/10.1016/j.electacta.2014.11.017.

15. A. R. Mainar, E. Iruin, L. C. Colmenares R., J. A. Blázquez, *Energy Sci. Eng*., **3**, 174 (2018). doi.org/10.1002/ese3.191
16. Z. Stoynov, D. Vladikova, B. Burdin, J. Laurencin, D. Montinaro, A. Nakajo, P. Picardo, A. Thorel, M. Hubert, R. Spotorno, A. Chesnaud, *MRS Advances*, **2**, 3991 (2017). doi.org/10.1557/adv.2017.592.
17. D. Vladikova, Z. Stoynov, G. Raikova in: Z. Stoynov, D. Vladikova (Eds.), Marin Drinov Academic Publishing House, Sofia, p.441 (ISBN 954-322-133-2) (2006).

СКРИНИНГОВ ИМПЕДАНСЕН АНАЛИЗ НА ЦИНК-ВЪЗДУШНИ КЛЕТКИ

З. Б. Стойнов[1†], Д. Е. Владикова1*, Б. И. Абрашев[1], М. П. Славова[1], Б. Г. Бурдин[1], Е. С. Михайлова-Димитрова[1], Л. К. Коменарес [2], А. Р. Мейнар [2], Ж. А. Блазкес [2]

[1]Институт по електрохимия и енергийни системи, Българска академия на науките, ул. Акад. Г. Бончев, бл. 10, София 1113, България
[2]CIDETEC Съхранение на енергия, Pº Мирамон 196, 20014 Сан Себастиан, Испания

Постъпила на 19 февруари, 2018 г.; приета на 2 март, 2018 г.

Като обещаваща технология, вторичните цинк-въздушни батерии спечелиха значително внимание през последните няколко години. Представената работа цели въвеждането на електрохимична импедансна спектроскопия (EIS) като инструмент за разработване на нови наноструктурирани и екологосъобразни материали, подходящи за внедряване в акумулаторна цинк-въздушна клетка. Първите резултати при циклиране са получени при измервания както в конфигурация на полу-клетка, така и на цяла клетка. Те осигуряват електрохимично охарактеризиране на клетката и нейните компоненти (електроди и електролит) при фиксирано състояние на заряд, което позволява експериментално дефиниране на скорост-определящия стадий. Получената информация ще бъде използвана за по-нататъшно проучване и оптимизиране на цинк-въздушната клетка.